

ARTICLE

Received 30 Aug 2013 | Accepted 1 Apr 2014 | Published 29 Apr 2014

DOI: 10.1038/ncomms4776

OPEN

Faster growth of the major prokaryotic versus eukaryotic CO₂ fixers in the oligotrophic ocean

Mikhail V. Zubkov¹

Because maintenance of non-scalable cellular components—membranes and chromosomes—requires an increasing fraction of energy as cell size decreases, miniaturization comes at a considerable energetic cost for a phytoplanktonic cell. Consequently, if eukaryotes can use their superior energetic resources to acquire nutrients with more or even similar efficiency compared with prokaryotes, larger unicellular eukaryotes should be able to achieve higher growth rates than smaller cyanobacteria. Here, to test this hypothesis, we directly compare the intrinsic growth rates of phototrophic prokaryotes and eukaryotes from the equatorial to temperate South Atlantic using an original flow cytometric ¹⁴CO₂-tracer approach. At the ocean basin scale, cyanobacteria double their biomass twice as frequently as the picoeukaryotes indicating that the prokaryotes are faster growing CO₂ fixers, better adapted to phototrophic living in the oligotrophic open ocean—the most extensive biome on Earth.

¹Ocean Biogeochemistry & Ecosystems Research Group, National Oceanography Centre, European Way, Southampton SO14 3ZH, UK. Correspondence and requests for materials should be addressed to M.V.Z. (email: mvz@noc.ac.uk).

Since the beginning of life on Earth, prokaryotes have regulated the main global biogeochemical cycles^{1,2}. However, after the energetically superior eukaryotes³ had evolved, prokaryotes appeared to lose control over biological CO₂ fixation in all major biomes including the open ocean. Apparently non-scalable cellular components such as chromosomes and membranes handicap growth rates of the smaller phytoplankton cells (cell diameter ~1 µm) relative to larger cells (cell diameter 4–8 µm)^{4,5}. There is supporting field evidence that phototrophic picoeukaryotes dominate over cyanobacteria in primary production in coastal⁶ and certain oceanic regions^{7,8}. On the other hand the above handicap could be counterbalanced by nutrient transport efficiency, which decreases with increase in cell size^{9,10}.

Direct comparison of *in situ* growth rates of phototrophic prokaryotes and eukaryotes in the oceanic subtropical gyres can show whether prokaryotes or picoeukaryotes are best adapted to oligotrophic conditions. Compared with other oceanic biomes these gyres are seasonally relatively stable and have remained steady for the geological time necessary for biological co-evolution of these organisms to occur. Because biomass growth of both groups primarily depends on photosynthesis, it is justifiable to compare their growth using the CO₂ fixation rates. Until now, cellular biomass of oceanic microbes has been calculated from biovolume, determined microscopically⁸, or using a change in impedance⁶ or by size fractionation¹¹, and multiplied by a poorly constrained volume-to-carbon conversion factor, derived from culture studies¹², under an assumption that the factor is unaffected by growth conditions.

Here, to circumvent the above assumption, a ¹⁴C-tracer experimental method, in which cumulative cellular CO₂ fixation was determined at the end of the light period (12 h) and at the end of the following 12-h dark period (24 h), is developed to compare growth and biomass of the smallest oceanic plastidic protists and cyanobacteria. We find that cyanobacteria grow twice as fast as the smallest eukaryotes both in the South Atlantic gyre and in adjacent regions. Despite their protracted co-evolution simple prokaryotic CO₂ fixers outgrow complex eukaryotic CO₂ fixers in the oligotrophic gyre ecosystems highlighting the under-rated growth capacity of phototrophic prokaryotes.

Results

Prokaryotic and eukaryotic groups examined for CO₂ fixation.

Sixteen experiments were completed in the South Atlantic Ocean in three oceanic regions: the Equatorial convergence region (EQ), Southern subtropical gyre (SG) and Southern temperate region (ST) (Supplementary Fig. 1) to compare representative mean growth rates that should encompass natural variations in cell abundance and nutrient availability. The following cells were flow sorted: *Prochlorococcus* (*Pro*)¹³, *Synechococcus* (*Syn*), small plastidic protists (PI-S, cell diameter ~2 µm), large plastidic protists (PI-L, cell diameter ~3 µm)^{8,14,15}. In addition, low-nucleic acid (LNA)-containing bacterioplankton and aplastidic protists (A-PI, cell diameter ~3 µm) were flow sorted as controls.

To compare cellular growth and biomass of the smallest oceanic plastidic protists and cyanobacteria, ¹⁴CO₂ fixation by flow cytometrically enumerated and sorted *Pro*, *Syn*, PI-S and PI-L cells was measured at the end of the light period (12 h) and at the end of the following 12-h dark period (24 h). The amount of tracer in flow-sorted *Pro*, *Syn*, PI-S and PI-L cells was generally higher at 12 h than at 24 h, while the opposite was true for A-PI cells (Supplementary Figs 2 and 3). The amount of tracer in flow-sorted LNA cells was statistically indistinguishable from the background (Supplementary Fig. 3), indicating that the SAR11 alphaproteobacteria, which comprised the LNA cell population¹³,

did not fix CO₂. The increased ¹⁴C-radioactivity of the A-PI cells in the dark has a ready explanation—the A-PI cells continued feeding on ¹⁴C-labelled CO₂ fixers in the dark. The decreased ¹⁴C-radioactivity of the *Pro*, *Syn*, PI-S and PI-L cells in the dark (Supplementary Fig. 2b–f) can depend on two cellular processes. First, the cells had directly lost carbon fixed during the light period (primarily by respiration but also exudation, egestion or lysis). Second, the reduction in cellular radioactivity was a result of cell division, because smaller daughter cells would contain less tracer than the larger parent cells and therefore an increased proportion of daughter cells will decrease average radioactivity per cell in the sampled population.

Dark respiration versus cell division. To assess the magnitude of dark physiological loss of ¹⁴C, tracer retention by each population as well as by their sum was compared at 12 and 24 h (Supplementary Fig. 4). Average cellular ¹⁴C content was multiplied by corresponding cell concentrations (Supplementary Fig. 5). A statistically significant increase in radioactivity of the A-PI population between 12 and 24 h (Supplementary Fig. 4b) was a result of A-PI cells feeding on ¹⁴C-labelled phototrophic cells in the dark. No statistically significant difference in the *Pro*, PI-S and PI-L populations was found between the two time points indicating that dark respiration of ¹⁴C-labelled material in those cells was insignificant. Statistical significance of the decrease in the radioactivity of the *Syn* population (Supplementary Fig. 4e) was more likely due to grazing on *Syn* cells by A-PI, mixotrophic PI-S and PI-L cells^{14,15} than to *Syn* dark respiration, because the ¹⁴CO₂ fixed at 12 and 24 h by the sum of all flow-sorted populations (including predators) was similar (Supplementary Fig. 4a).

The above negligibly small dark respiration of ¹⁴C-labelled cellular material is in agreement with earlier laboratory experiments on algal cultures¹⁶ with dark respiration being 2–16% of daily fixed CO₂. A 12% value was calculated for nitrate-limited chemostat-growing cultures of *Monochrysis lutheri*¹⁷, when washout from a chemostat was taken into account. Relative dark respiration for a batch culture of *Isochrysis galbana* grown from nutrient-replete into nutrient-starved conditions was about 4%¹⁸. For *Skeletonema costatum* grown under nutrient-replete conditions at photon flux densities of 50 and 1,200 µmol photons m⁻² s⁻¹ dark respiration was 2% and 16% of photosynthesis, respectively¹⁹. However, there were also reports of considerable dark respiration that accounted for 30–40% of daylight CO₂ fixation in oligotrophic waters²⁰ and 20–25% of daylight CO₂ fixation in the temperate North Atlantic²¹. The discrepancy between the reported high dark respiration and the presented data (Supplementary Fig. 4) presumably originated from the methodological differences. The published high values were obtained by gently collecting live phytoplankton on filters. In the present study, phytoplankton samples were fixed to preserve cell integrity for subsequent flow sorting. Only ¹⁴C tracer incorporated into macromolecules remained in fixed cells and ¹⁴C tracer incorporated into labile cellular material was released on fixation, whereas labelled labile material remained in the unfixed cells²². Labile material such as sugars is preferentially respired by cells²³, while turnover of labelled macromolecules in cells is slow²⁴. In the present study, the dark respiration of macromolecules was examined and found negligibly low (Supplementary Fig. 4), and hence cell division was considered as the main process responsible for radiotracer decrease in mean cells in the dark (Supplementary Fig. 2).

Pro and *Syn* as well as the smallest plastidic protists synchronize their cell division after dusk^{25–29} (M.V.Z., unpublished observations). Therefore assumption of

night cell division is plausible. This means that only the difference between divisions in the first 12 light hours and the subsequent 12 dark hours can be determined. Accordingly, the derived growth rates are conservative estimates.

Group-specific growth rates. The observed increases in concentrations of cells between 12 and 24 h (Supplementary Fig. 5) were used to independently assess group-specific growth rates for comparison with the rates determined using the ^{14}C tracer method. The growth rates of the PI-S and PI-L, estimated by the two methods, were statistically similar (Supplementary Fig. 6), proving that the tracer method gave realistic estimates of growth rates of plastidic protists.

The tracer-derived growth rates of the *Pro* and *Syn* were 2–4 times higher than their cell-derived growth rates. This discrepancy can be reconciled if cyanobacteria either have high rates of dark respiration, or are under strong mortality pressure. In the first case, mean dark respiration should be $>50\%$ for *Pro* and *Syn* in the SG + EQ and EQ, respectively, and 80% for *Syn* in the ST. These high values are unlikely (see above, Supplementary Fig. 4e,f). The increased radioactivity of the A-PI in the dark (Supplementary Figs 2a and 4b), and similar radioactivity of the sum (Supplementary Fig. 4a) support grazing on cyanobacteria by the A-PI, PI-L and PI-S. Those grazing-related ^{14}C retentions would reduce the tracer-based estimates of growth rates of PI-S and PI-L. Indeed, their tracer-derived growth rates showed a trend of being lower than their cell-derived growth rates (Supplementary Fig. 6); however, the differences were statistically insignificant, suggesting that phototrophic CO_2 fixation is the main contributor to the growth of PI-L and PI-S cells. Accordingly, grazing being the main cause of the difference between the tracer-derived and cell-derived growth rates of the *Pro* and *Syn* (Supplementary Fig. 6), the former estimated the intrinsic growth of cyanobacteria, whereas the latter estimated the net growth of cyanobacteria.

Comparison of the growth rates of the CO_2 fixers. The region-averaged growth rates of the studied groups ranged between 0.1 and 0.6 d^{-1} (Fig. 1). The *Syn* grew fastest in the EQ regions, 0.7 d^{-1} ; however, these data were omitted from the figure as unrepresentative for the combined EQ + SG regions, because *Syn* growth was not determined in the SG region owing to their low

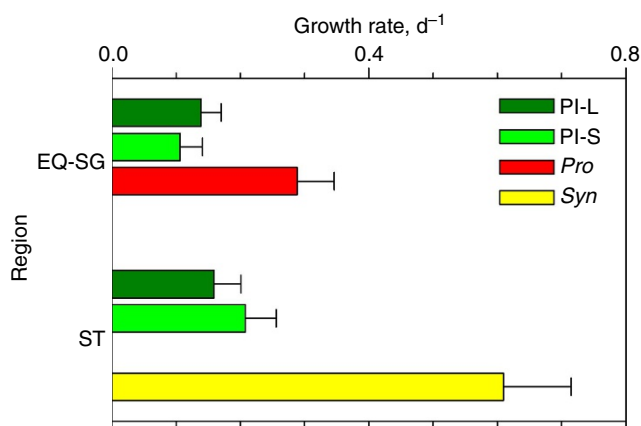


Figure 1 | Relative growth rates of phytoplankton groups. Comparison of the growth rates of large plastidic protists (PI-L), small plastidic protists (PI-S), *Prochlorococcus* (*Pro*) and *Synechococcus* (*Syn*) in the two regions: combined Equatorial waters (EQ) and Southern gyre (SG) and Southern temperate waters (ST). Error bars indicate propagated single s.e.

cell concentrations (Supplementary Fig. 1b). The growth rates of *Pro* in the EQ ($0.3\text{--}0.6\text{ d}^{-1}$) are similar to *Pro* growth rates determined at the base of the photic layer in the Sargasso Sea³⁰ and in agreement with rates of up to one doubling per day, determined in the equatorial Pacific using cell cycle analysis²⁵. The mean growth rates of *Syn* in the ST and *Pro* in the EQ + SG were, respectively, three and two times higher than the mean growth rates of PI-L or PI-S (Supplementary Fig. 6). Therefore, the growth rates of both cyanobacteria in all regions studied were significantly higher than the growth rates of the smallest plastidic protists.

The finding that plastidic protists have lower growth rates than cyanobacteria (Fig. 1) requires reconciliation with the hypothesis of optimal cell size to achieve maximum photosynthetic growth^{4,5}. In the present study, the smallest eukaryotes showed growth rates (Fig. 1; Supplementary Fig. 6) of one half or less compared with the growth rates of eukaryotes of comparable size in nutrient-rich culture⁵. If the taxon-independent approach is applied, the above suggests that eukaryotes are underperforming in the oligotrophic open ocean, being poorly adapted to their habitat. An alternative explanation could be that the eukaryotes cultured in the laboratory are physiologically different from the eukaryotes inhabiting the open ocean, for example, the latter are mixotrophs under-represented in culture collections but capable of outcompeting obligate phototrophs in nature³¹. If this is correct, the difference between potential and realized growth rates is as likely to be related to physiological divergence as to evolutionary inadequacy.

There is more controversy about the *in situ* growth rates of the *Pro* and *Syn* in the EQ (Figs 1 and 2; Supplementary Fig. 6) being about twice as high as their growth rates in the nutrient unlimited culture at similar light intensity⁵. Because the *in situ* rates cannot be higher than the maximum rates, it is probable that either low temperature of 18°C or high nutrient conditions in culture experiments were less optimal for the cyanobacterial growth than the low nutrient conditions in the open ocean.

Fixation rates and biomasses of the CO_2 fixers. The cellular CO_2 fixation rates of the studied groups span four orders of magnitude

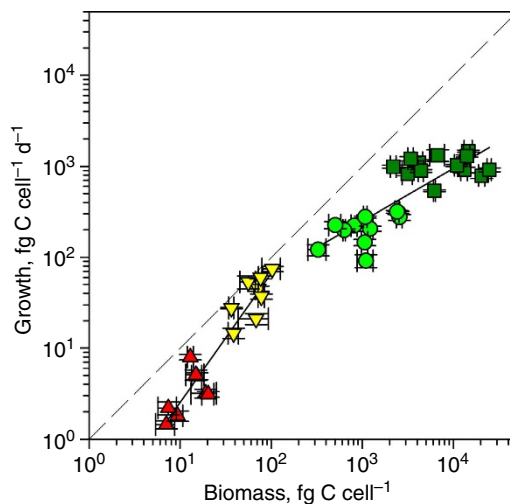


Figure 2 | Metabolic scaling in prokaryotes and eukaryotes. Scatter plot of biomass versus daily growth of *Prochlorococcus* (red triangles), *Synechococcus* (yellow triangles), small plastidic protists (green circles) and large plastidic protists (green squares) to compare their growth. Solid lines indicate linear regressions of cyanobacteria (slope = 1.4, $r^2 = 0.89$, $P < 0.001$) and picoeukaryotes (slope = 0.6, $r^2 = 0.67$, $P < 0.001$). Dashed line indicates equality of biomass and daily growth.

in direct proportion to their cellular biomasses (Fig. 3a). The average fixation rates of the PI-L and PI-S cells were statistically similar in all regions and the average fixation rates of the *Syn* cells were comparable in the EQ and ST regions. Being more sensitive to nutrient conditions, the cellular CO₂ fixation rates of cyanobacteria were more variable than the rates of eukaryotes (Supplementary Fig. 2).

The average biomass of *Pro* and *Syn* cells was 60% lower and the biomass of PI-S and PI-L was 20–120% higher according to the tracer method compared with the biovolume method^{11,15} (Fig. 3a). First, it was reassuring that the estimates based on the two independent approaches were comparable. Second, because *Pro* and *Syn* cell diameters were estimated by size fractionation using broad-stepped (0.2 μm) pore size filters it was unsurprising that the biovolume-based method gave higher biomass estimates. Third, the microscopic size measurements of fixed and consequently shrunk PI-S and PI-L cells using nucleic acid-specific stain would underestimate the living cell sizes. Hence, cellular biomass, estimated using the sensitive ¹⁴C-tracer method, is more likely to be closer to the real biomass of living cells. Among the studied groups *Pro* cells were the smallest (Fig. 3a). Taking a 1.7-Mbp genome size of *Pro* MED4 strain for guidance³², the *Pro* chromosome would constitute 5% of cellular biomass, which is within the theoretical limits⁴ for a viable phototrophic cell.

Within the limited size range of the studied microbes a relationship between the cellular biomass and biomass growth rate indicates a slope difference between the cyanobacteria and smallest plastidic protists (Fig. 2). The slope drop from prokaryotes to eukaryotes is in agreement with the step shift during a transition from heterotrophic prokaryotes to protozoa³³, suggesting similarity in bioenergetic scaling between phototrophic and heterotrophic microbes. Such similarity could be linked to commonness of versatile metabolism among oceanic CO₂-fixing microbes—mixotrophy of the smallest eukaryotes¹⁵ and photoheterotrophy of cyanobacteria¹³.

At the population level the biomasses of the *Pro* and *Syn* were, respectively, 40% and 20% of the biomass of the PI-L (Fig. 3b), or merely 25% of the sum of PI-L, PI-S and *Pro* in the EQ + SG and 13% of PI-L, PI-S and *Syn* in the ST. Daily CO₂ fixation by the *Pro* and *Syn* populations equated to 80% of the fixation by the PI-L population, or 40 and 35% by the corresponding sums. Although eukaryotes clearly dominated the biomass of the CO₂ fixers in the studied regions, cyanobacterial populations fixed CO₂ more effectively and grew faster. If grazing control by eukaryotes was relaxed, cyanobacterial populations could outgrow populations of plastidic protists within days because of faster cyanobacterial reproduction.

Discussion

It seems that after >10⁹ years of co-evolution³⁴ the smallest phototrophic eukaryotes have not succeeded in exceeding the growth of cyanobacteria in the oligotrophic open ocean. However, if, in addition to competing for major inorganic nutrients, eukaryotes feed on bacteria^{14,35,36}, then eukaryote survival as predators would depend on growth of phototrophic prokaryotes. The nutritional adaptations of phototrophic eukaryotes and prokaryotes in the nutrient-depleted open ocean have established, perhaps, the simplest ecosystem of faster growing photoheterotrophic prokaryotes largely controlled by mixotrophic eukaryotes.

Methods

Sampling. The experimental study was carried out on board the UK Royal Research Ship *James Cook* during the Atlantic Meridional Transect (AMT) cruise number JC079 (AMT22) in October–November 2012. Seawater samples were

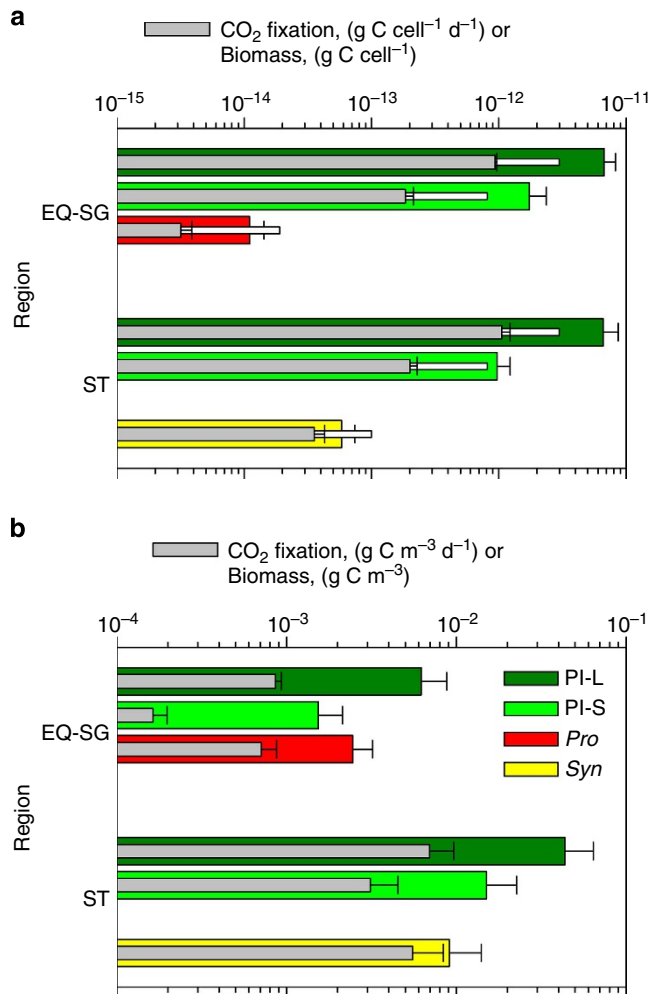


Figure 3 | Absolute biomasses and growth rates of phytoplankton groups. Comparison of the ¹⁴C tracer-based estimates of cellular (a) and population (b) biomasses and growth rates (internal intermediate grey bars) of large plastidic protists (PI-L), small plastidic protists (PI-S), *Prochlorococcus* (*Pro*) and *Synechococcus* (*Syn*) in the two regions: combined Equatorial waters (EQ) and Southern gyre (SG) and Southern temperate waters (ST). Thin white bars (a) indicate biovolume-based estimates of cellular biomass. Note the log scale of the x axis. Error bars indicate propagated single s.e.

collected before dawn with 20-litre Niskin bottles mounted on the sampling rosette of a conductivity-temperature-depth (CTD) profiler (Sea-Bird Electronics, Washington, USA) from a depth of 20 m, a representative depth of the surface mixed layer unaffected by the ship's movement and contamination. Samples were gently transferred into a 10-l polypropylene carboy, before being dispensed through a spigot into 120-ml Pyrex glass bottles. All plastic and glasswares were soaked in 10% HCl and extensively rinsed with sampled seawater. All experiments were set up within 20 min after sample collection.

CO₂ fixation experiments. To assess the effect of high NaH¹⁴CO₃ tracer addition, necessary to determine CO₂ fixation rates by the tiniest phototrophic prokaryote—*Pro* cyanobacteria³⁰, radiotracers of two manufacturers were used. Sodium bicarbonate as a solution (Perkin-Elmer, USA) was added directly to sampled seawater, while crystals of sodium bicarbonate (Hartmann Analytic, Germany), were dissolved in autoclaved seawater, collected from 20 m depth (the latter tracer gave on average 12% higher estimates of CO₂ fixation than the former one—data not shown). Working solutions of both radiotracers were filtered through a 0.2-μm pore size filter before being added to sampled seawater (90–240 kBq ml⁻¹ final radioactivity). The bottled samples were then incubated at ambient temperatures controlled by a refrigerated water bath (Grant Instruments, UK) in a 6-l acrylic glass water tank illuminated by a warm white light-emitting diode array (Photon Systems Instruments, Czech Republic) adjusted to 350 μmol photons m⁻² s⁻¹,

mimicking the average *in situ* light conditions at 20 m depth in subtropical waters. The constant light output was used to allow direct comparison of cellular CO₂ fixation determined in experiments with seawater samples collected at different latitudes. After 12 h incubation in the light, to mimic the day period, 60 ml of sample were poured into a polypropylene bottle containing 3 ml of 20% paraformaldehyde (PFA, final concentration 1%). PFA solution was prepared by dissolving PFA powder in seawater by stirring on a heating plate followed by filtering of cooled solution through a 0.2-µm pore size filter. The Pyrex bottles containing the remaining 60 ml of sample were transferred into a parallel, temperature-controlled, light-tight 6-l tank and incubated for an additional 12 h in the dark at ambient temperature to mimic the night period. At the end of the experiment, the remaining 60 ml of sample were fixed with 1% PFA. CO₂ fixation in dark controls were <2% of CO₂ fixation in the 12-h light incubations (for example, 0.18 ± 0.01 mg C m⁻³ d⁻¹ in the dark versus 9.68 ± 0.84 mg C m⁻³ d⁻¹ in the light at 4°1.8'N, 26°28.2'W).

Subsamples were taken from each polypropylene bottle containing a fixed sample to determine the total CO₂ fixation and the exact amount of added radiotracer. Three 1.6-ml subsamples were transferred into 2-ml microcentrifuge tubes to determine absolute concentrations of microbial populations (see below) and to flow sort *Pro* cells, when their natural abundance was sufficiently high to sort at a rate of 150–300 cells min⁻¹. A single 20-ml subsample was concentrated using a 0.4-µm polycarbonate filter (Nuclepore, Whatman, UK) mounted on a filtration unit (Swinnex, Millipore, USA) using a syringe pump (KD Scientific, USA) at a flow rate of 2.0 ml min⁻¹ and used for sorting stained *Pro* and *Syn* cells as well as Pl-S. The remaining sample was concentrated using a 0.6-µm Nuclepore polycarbonate filter in the same way for flow sorting Pl-L and A-Pl. The seawater retained inside the filtration units as well as the filters were transferred into 2-ml microcentrifuge tubes. The unconcentrated subsamples and two concentrated subsamples of the same 1.6-ml final volume, were stained inside the microcentrifuge tubes with SYBR Green I (Sigma-Aldrich, UK) in three potassium citrate buffer^{37,38} and flow sorted within 24 h. Stained samples scheduled for sorting were stored in the dark at 4 °C.

Flow cytometric sorting. Stained microbial cells from different populations were discriminated, enumerated and flow sorted using a FACSCalibur flow cytometer (Becton Dickinson, Oxford, UK). An internal standard of 0.5 and 1.0 µm diameter, multi-fluorescent beads (Polysciences, Germany) was added to each stained sample before analyses to monitor instrument performance and to determine absolute concentrations of microbial populations^{38,39}.

For each flow-sorted population 4–6 replicates of different cell numbers were sorted (for example, Supplementary Fig. 3). Bacterial and eukaryotic cells were collected on 0.2 and 0.8-µm polycarbonate filters, respectively, using a three-socket filtration unit and prepared for radio-assaying following the same procedure as for total carbon fixation measurements. Using a liquid scintillation counter (Tri-Carb 3100, Perkin Elmer, UK), samples (a sample was counted for 5 min) from each experiment were batch counted 3–4 times on different days. To account for counting variations a mean of these 3–4 counts was calculated before a relative average cellular rate of CO₂ fixation was computed as a fraction of the amount of radiotracer added to the experimental bottle. To enable comparison of measured cellular CO₂ fixation rates between experiments, absolute fixation rates were calculated.

CO₂ concentrations in sampled seawater, derived from the CTD measurements of seawater salinity⁴⁰ were used to convert relative cellular rates of CO₂ fixation into absolute CO₂ fixation rates in units of gram carbon fixed by an average cell of the flow-sorted population. The CO₂ fixation of flow-sorted *Pro*, *Syn*, Pl-S or Pl-L cells was determined experimentally as a mean cellular daily growth rate C_{12}^{fix} (g C cell⁻¹ d⁻¹). The CO₂ fixation C_{24}^{fix} , determined at 24 h, is a mean for the fraction of cells that divided during the dark period (D^{div}) and the ones that remained undivided. The divided cells double in number but each cell contains a half of the fixed CO₂. This simple model can be described by the following formula:

$$C_{24}^{fix} = (2 \times D^{div} \times C_{12}^{fix} / 2 + (1 - D^{div}) \times C_{12}^{fix}) / (1 + D^{div}) \quad (1)$$

The above formula can be simplified and re-arranged to calculate the daily relative growth rate D^{div} [d⁻¹] assuming that cells divided during the dark period:

$$D^{div} = (C_{12}^{fix} - C_{24}^{fix}) / C_{24}^{fix} \quad (2)$$

Then the cellular biomass C^{biom} (g C cell⁻¹) could be computed:

$$C^{biom} = C_{12}^{fix} / D^{div} \quad (3)$$

or

$$C^{biom} = C_{12}^{fix} \times C_{24}^{fix} / (C_{12}^{fix} - C_{24}^{fix}) \quad (4)$$

The F-test was used for analyses of variance and the paired *t*-test was used for comparing means or alternatively Wilcoxon's signed rank test was used in cases when the normality test failed ($P < 0.05$). s.e. of mean were propagated when growth rates, biomasses and population-specific CO₂ fixation rates were calculated.

References

- Kirchman, D. L. Carbon cycle—microbial breathing lessons. *Nature* **385**, 121–122 (1997).
- Falkowski, P. G., Fenchel, T. & Delong, E. F. The microbial engines that drive Earth's biogeochemical cycles. *Science* **320**, 1034–1039 (2008).
- Lane, N. & Martin, W. The energetics of genome complexity. *Nature* **467**, 929–934 (2010).
- Raven, J. A. Why are there no picoplanktonic O₂ evolvers with volumes less than 10⁻¹⁹ M³? *J. Plankton Res.* **16**, 565–580 (1994).
- Maranon, E. *et al.* Unimodal size scaling of phytoplankton growth and the size dependence of nutrient uptake and use. *Ecol. Lett.* **16**, 371–379 (2013).
- Worden, A. Z., Nolan, J. K. & Palenik, B. Assessing the dynamics and ecology of marine picophytoplankton: the importance of the eukaryotic component. *Limnol. Oceanogr.* **49**, 168–179 (2004).
- Li, W. K. W. Primary production of prochlorophytes, cyanobacteria, and eukaryotic ultraphytoplankton—measurements from flow cytometric sorting. *Limnol. Oceanogr.* **39**, 169–175 (1994).
- Jardillier, L., Zubkov, M. V., Pearman, J. & Scanlan, D. J. Significant CO₂ fixation by small prymnesiophytes in the subtropical and tropical northeast Atlantic Ocean. *ISME J.* **4**, 1180–1192 (2010).
- Chisholm, S. W. in *Primary Productivity and Biogeochemical Cycles in the Sea* (eds Falkowski, P. G. & Woodhead, A. D.) 213–237 (Plenum, 1992).
- Banavar, J. R., Damuth, J., Maritan, A. & Rinaldo, A. Supply-demand balance and metabolic scaling. *Proc. Natl Acad. Sci. USA* **99**, 10506–10509 (2002).
- Zubkov, M. V., Sleight, M. A., Burkill, P. H. & Leakey, R. J. G. Picoplankton community structure on the Atlantic Meridional Transect: a comparison between seasons. *Prog. Oceanogr.* **45**, 369–386 (2000).
- Christian, J. R. & Karl, D. M. Microbial community structure at the United-States Joint Global Ocean Flux Study Station ALOHA—inverse methods for estimating biochemical indicator ratios. *J. Geophys. Res.* **99**, 14269–14276 (1994).
- Gomez-Pereira, P. R. *et al.* Comparable light stimulation of organic nutrient uptake by SAR11 and *Prochlorococcus* in the North Atlantic subtropical gyre. *ISME J.* **7**, 603–614 (2013).
- Zubkov, M. V. & Tarran, G. A. High bacterivory by the smallest phytoplankton in the North Atlantic Ocean. *Nature* **455**, 224–226 (2008).
- Hartmann, M. *et al.* Mixotrophic basis of Atlantic oligotrophic ecosystems. *Proc. Natl Acad. Sci. USA* **109**, 5756–5760 (2012).
- Geider, R. J. & Osborne, B. A. Respiration and microalgal growth—a review of the quantitative relationship between dark respiration and growth. *New Phytol.* **112**, 327–341 (1989).
- Laws, E. & Caperon, J. Carbon and nitrogen metabolism by *Monochrysis lutheri*—measurement of growth rate dependent respiration rates. *Mar. Biol.* **36**, 85–97 (1976).
- Flynn, K. J., Davidson, K. & Leftley, J. W. Carbon-nitrogen relations at whole-cell and free-amino-acid levels during batch growth of *Isochrysis galbana* (Prymnesiophyceae) under conditions of alternating light and dark. *Mar. Biol.* **118**, 229–237 (1994).
- Anning, T. *et al.* Photoacclimation in the marine diatom *Skeletonema costatum*. *Limnol. Oceanogr.* **45**, 1807–1817 (2000).
- Geider, R. J. in *Primary Productivity and Biogeochemical Cycles in the Sea* (ed. Falkowski, P.) 333–360 (Plenum, 1992).
- Marra, J. & Barber, R. T. Phytoplankton and heterotrophic respiration in the surface layer of the ocean. *Geophys. Res. Lett.* **31**, L09314 (2004).
- Zubkov, M. V. & Leakey, R. J. G. Evaluation of the efficiency of metabolism of dinoflagellate phosphorus and carbon by a planktonic ciliate. *Eur. J. Protistol.* **45**, 166–173 (2009).
- Glover, H. E. & Morris, I. Photosynthetic characteristics of coccoid marine cyanobacteria. *Arch. Microbiol.* **129**, 42–46 (1981).
- Zubkov, M. V., Sleight, M. A. & Burkill, P. H. Measurement of bacterivory by protists in open ocean waters. *FEMS Microbiol. Ecol.* **27**, 85–102 (1998).
- Vaulot, D., Marie, D., Olson, R. J. & Chisholm, S. W. Growth of *Prochlorococcus*, a photosynthetic prokaryote, in the equatorial Pacific Ocean. *Science* **268**, 1480–1482 (1995).
- Vaulot, D. & Marie, D. Diel variability of photosynthetic picoplankton in the equatorial Pacific. *J. Geophys. Res.* **104**, 3297–3310 (1999).
- Wyman, M. Diel rhythms in ribulose-1,5-bisphosphate carboxylase/oxygenase and glutamine synthetase gene expression in a natural population of marine picoplanktonic cyanobacteria (*Synechococcus* spp.). *Appl. Environ. Microbiol.* **65**, 3651–3659 (1999).
- Zubkov, M. V., Sleight, M. A. & Burkill, P. H. Assaying picoplankton distribution by flow cytometry of underway samples collected along a meridional transect across the Atlantic Ocean. *Aquat. Microb. Ecol.* **21**, 13–20 (2000).
- Zubkov, M. V. & Quartly, G. D. Ultraplankton distribution in surface waters of the Mozambique Channel—flow cytometry and satellite imagery. *Aquat. Microb. Ecol.* **33**, 155–161 (2003).

30. Chisholm, S. W. *et al.* A novel free-living prochlorophyte abundant in the oceanic euphotic zone. *Nature* **334**, 340–343 (1988).
31. Tittel, J. *et al.* Mixotrophs combine resource use to outcompete specialists: Implications for aquatic food webs. *Proc. Natl Acad. Sci. USA* **100**, 12776–12781 (2003).
32. Rocop, G. *et al.* Genome divergence in two *Prochlorococcus* ecotypes reflects oceanic niche differentiation. *Nature* **424**, 1042–1047 (2003).
33. DeLong, J. P., Okie, J. G., Moses, M. E., Sibly, R. M. & Brown, J. H. Shifts in metabolic scaling, production, and efficiency across major evolutionary transitions of life. *Proc. Natl Acad. Sci. USA* **107**, 12941–12945 (2010).
34. Knoll, A. H., Javaux, E. J., Hewitt, D. & Cohen, P. Eukaryotic organisms in Proterozoic oceans. *Philos. Trans. R. Soc. Lond. B Biol. Sci.* **361**, 1023–1038 (2006).
35. Frias-Lopez, J., Thompson, A., Waldbauer, J. & Chisholm, S. W. Use of stable isotope-labelled cells to identify active grazers of picocyanobacteria in ocean surface waters. *Environ. Microbiol.* **11**, 512–525 (2009).
36. Hartmann, M., Zubkov, M. V., Scanlan, D. J. & Lepere, C. In situ interactions between photosynthetic picoeukaryotes and bacterioplankton in the Atlantic Ocean: evidence for mixotrophy. *Environ. Microbiol. Rep.* **5**, 835–840 (2013).
37. Marie, D., Partensky, F., Jacquet, S. & Vault, D. Enumeration and cell cycle analysis of natural populations of marine picoplankton by flow cytometry using the nucleic acid stain SYBR Green I. *Appl. Environ. Microbiol.* **63**, 186–193 (1997).
38. Zubkov, M. V., Burkill, P. H. & Topping, J. N. Flow cytometric enumeration of DNA-stained oceanic planktonic protists. *J. Plankton Res.* **29**, 79–86 (2007).
39. Zubkov, M. V. & Burkill, P. H. Syringe pumped high speed flow cytometry of oceanic phytoplankton. *Cytometry A* **69**, 1010–1019 (2006).
40. Parsons, T. R., Maita, Y. & Lalli, C. M. *Manual of chemical and biological methods for seawater analysis* (Pergamon, 1984).

Acknowledgements

I thank Glen Tarran (the chief scientist), fellow scientists, technicians, captain, officers and crew aboard the RRS *James Cook* for their support during the cruise. I gratefully acknowledge Michael Sleigh, Richard Geider and Adrian Martin for their critical comments on earlier drafts of the paper. This study was supported by the UK Natural Environment Research Council (NERC) through the core funding of the National Oceanography Centre as well as through the Research Grant NE/H005196/1, and the European Commission Seventh Framework Programme through the GreenSeas Collaborative Project (FP7-ENV-2010 Contract 265294). This is Atlantic Meridional Transect publication number 248.

Additional information

Supplementary information accompanies this paper at <http://www.nature.com/naturecommunications>

Competing financial interests: The author declares no competing financial interests.

Reprints and permission information is available online at <http://npg.nature.com/reprintsandpermissions>

How to cite this article: Zubkov, M. V. Faster growth of the major prokaryotic versus eukaryotic CO₂ fixers in the oligotrophic ocean. *Nat. Commun.* **5**:3776 doi: 10.1038/ncomms4776 (2014).



This work is licensed under a Creative Commons Attribution 3.0 Unported License. The images or other third party material in this article are included in the article's Creative Commons license, unless indicated otherwise in the credit line; if the material is not included under the Creative Commons license, users will need to obtain permission from the license holder to reproduce the material. To view a copy of this license, visit <http://creativecommons.org/licenses/by/3.0/>